Pharmacological Research 192 (2023) 106781

Contents lists available at ScienceDirect

Pharmacological Research

journal homepage: www.elsevier.com/locate/yphrs

Improving the tumor selectivity of T cell engagers by logic-gated dual tumor-targeting

Ying Shen [a,b,1], Shi-jie Jin [a,1], Yi-chang Chen [a], Wen-hui Liu [a,d], Yi-ming Li [a], Wen-yi Zhao [a,b], Ying-chun Xu [a], Shu-qing Chen [a,*], Wen-bin Zhao [a,b,c,**]

[a] Institute of Drug Metabolism and Pharmaceutical Analysis & Zhejiang Provincial Key Laboratory of Anti-Cancer Drug Research, College of Pharmaceutical Sciences, Zhejiang University, Hangzhou 310058, China
[b] Innovation Institute for Artificial Intelligence in Medicine, Zhejiang University, Hangzhou 310018, China
[c] Key Laboratory of Prevention, Diagnosis and Therapy of Upper Gastrointestinal Cancer of Zhejiang Province, Hangzhou 310022, China
[d] Hangzhou Biosun Pharmaceutical Co., Ltd, Hangzhou 310015, China

ARTICLE INFO

Keywords:
Trispecific T cell engagers
Tumor selectivity
Dual tumor-targeting
Logic-gate
Interdomain configurations

ABSTRACT

Targeting single tumor antigens makes it difficult to provide sufficient tumor selectivity for T cell engagers (TCEs), leading to undesirable toxicity and even treatment failure, which is particularly serious in solid tumors. Here, we designed novel trispecific TCEs (TriTCEs) to improve the tumor selectivity of TCEs by logic-gated dual tumor-targeting. TriTCE can effectively redirect and activate T cells to kill tumor cells (~18 pM EC_{50}) by inducing the aggregation of dual tumor antigens, which was ~70- or 750- fold more effective than the single tumor-targeted isotype controls, respectively. Further *in vivo* experiments indicated that TriTCE has the ability to accumulate in tumor tissue and can induce circulating T cells to infiltrate into tumor sites. Hence, TriTCE showed a stronger tumor growth inhibition ability and significantly prolonged the survival time of the mice. Finally, we revealed that this concept of logic-gated dual tumor-targeted TriTCE can be applied to target different tumor antigens. Cumulatively, we reported novel dual tumor-targeted TriTCEs that can mediate a robust T cell response by simultaneous recognition of dual tumor antigens at the same cell surface. TriTCEs allow better selective T cell activity on tumor cells, resulting in safer TCE treatment.

1. Introduction

T cell engagers (TCEs) can retarget T cells to kill tumor cells, and their efficacy has been demonstrated in many preclinical and clinical studies [1,2]. However, the tumor antigens targeted by TCEs are often insufficient to distinguish tumor cells from healthy tissues, leading to on-target off-tumor toxicity in the clinical application of TCEs [3–5], which narrows the treatment window or even results in treatment failure. Due to the better reproducibility of blood cells, the human body has a relatively higher tolerance for hemocytotoxicity caused by TCEs in the treatment of hematologic tumors, which are the main indications for TCEs [1,6]. In contrast, antigen targets commonly used in solid tumors are often expressed in some important and unrenewable tissues or organs, whose engagement is likely to entail serious or even lethal adverse events [4,7]. Hence, sufficient tumor selectivity may reduce the undesirable toxicity of TCEs on healthy cells, thereby expanding their clinical indications.

Although targeting tumor-specific antigens can effectively improve

Abbreviations: ATCC, American Type Culture Collection; EC_{50}, concentration for 50% of maximal effect; FBS, fetal bovine serum; FRET, fluorescence resonance energy transfer; HEK293F, human embryonic kidney 293 F cells; HEK293T, human embryonic kidney 293 T cells; HLA, human leukocyte antigen; IFN-γ, Interferon γ; IL-2, Interleukin 2; LDH, lactate dehydrogenase; MFI, mean fluorescence intensity; PBMCs, peripheral blood mononuclear cells; pHLA, peptides presented by human leukocyte antigen; RMF/A2, RMFPNAPYL/HLA-A* 02:01; SLL/A2, SLLMWITQC/HLA-A* 02:01; TAA, tumor-associated antigen; TCEs, T cell engagers; TCR, T cell receptor; TCRm, TCR-mimic antibody; TriTCEs, trispecific T cell engagers.

* Correspondence to: College of Pharmaceutical Sciences, Zhejiang University, Hangzhou 310058, China.
** Corresponding author at: Institute of Drug Metabolism and Pharmaceutical Analysis & Zhejiang Provincial Key Laboratory of Anti-Cancer Drug Research, College of Pharmaceutical Sciences, Zhejiang University, Hangzhou 310058, China.
E-mail addresses: chenshuqing@zju.edu.cn (S.-q. Chen), pharmacy_zwb@zju.edu.cn (W.-b. Zhao).
[1] Authors are equal contributors.

https://doi.org/10.1016/j.phrs.2023.106781
Received 26 December 2022; Received in revised form 24 April 2023; Accepted 26 April 2023
Available online 28 April 2023

tumor selectivity, true tumor-specific antigens suitable for TCEs are rare. Interestingly, Oostindie et al. [8] demonstrated that targeting two different antigens expressed on the same tumor cell by logic-gated antibody pairs can enhance the functional selectivity of therapeutic antibodies. In addition, Banaszek et al. [9] designed two hemibodies to simultaneously bind their respective antigens on a single cell to induce reconstitution of anti-CD3 antibody on the tumor cell surface and proved that the reduction of nonspecific T cell activation in this logic-gated manner could effectively reduce the toxicity caused by TCEs. More directly, Tapia-Galisteo et al. [10] and Dicara et al. [11] revealed that dual tumor-targeted trispecific TCEs (TriTCEs) showed greater potency and specificity when compared to conventional single-targeting TCEs. This evidence demonstrated the potential advantages of logic-gated dual tumor-targeting, but designing therapeutic antibodies based on the above strategies required extremely high expression levels of both antigens.

Studies have suggested that interdomain configurations can influence the cytotoxicity of TCEs [5,12], and Santich et al. [12] discovered highly active TCEs with optimized interdomain spacing and spatial configuration. Therefore, we hypothesized that improving the tumor selectivity of TCEs by logic-gated dual tumor-targeting can be achieved by adjusting the interdomain spacing and spatial configuration. Here, we describe a novel type of dual tumor-targeted TriTCEs with the optimized spatial configuration that can induce potent antitumor activity if both antigens on the same tumor cell have been recognized, and the potency of TriTCEs was significantly reduced by single tumor-targeting of either antigen. In addition, the TCEs do not require a high level of antigen expression, which expands the options for selecting suitable antigens.

2. Materials and methods

2.1. Cells and culture conditions

Human embryonic kidney 293 F cells (HEK293F) were kindly provided by the Comprehensive AIDS Research Center (Tsinghua University), rotary cultured in SMM 293-TI medium (Sino Biological Inc.) supplemented with 0.5% fetal bovine serum (FBS; Gibco). Human melanoma cell line A375, human non-small cell lung cancer cell line PC9, human T lymphocyte cell line Jurkat, human peripheral blood B cell leukemia cell line BV173 and human erythroleukemic cell line K562 were purchased from American Type Culture Collection (ATCC), and maintained in RPMI-1640 (Gibco) with 10% FBS. Human embryonic kidney 293 T cells (HEK293T) were purchased from ATCC and maintained in DMEM (Gibco) with 10% FBS. Human ovarian cancer cell line SKOV3 was maintained in McCoy's 5 A modified medium (Thermo Fisher Scientific) with 10% FBS. Human peripheral blood mononuclear cells (PBMCs) were purchased from Milestone Biotechnologies(A10S04 5018), and rested in RPMI-1640 with 10% FBS for 4–12 before huse. All cells were maintained in media supplemented with 1% penicillin-streptomycin at 37 ℃ with 5% CO_2 and 95% humidity.

2.2. Design, construction, expression and purification of dual tumor-targeted TriTCE

The design of logic-gated dual tumor-targeted TriTCEs was based on the backbone of the conventional antibody IgG1. Briefly, two tumor antigen-binding domains were fused to the N-terminus of the two Fc arms in a Fab or TCR-fused (the β chain was fused with Fc, and the α chain was assembled with the β chain by a disulfide bond) format, respectively. To purify the correctly assembled protein, a 6 ×His tag was introduced into the C-terminus of Fc fused with the pHLA recognition arm, and a Flag tag was introduced into the C-terminus of another Fc. The anti-CD3 scFv was fused into the 3′ tail of the light chain (Fab) or α chain (TCR) of the pHLA-targeting part *via* a $(G_4S)_3$ linker. The genes of four chains assembled for each TriTCE were cloned into eukaryotic expression vectors after codon optimization to obtain four recombinant expression plasmids. TriTCEs were produced by transient transfection of four expression plasmids into HEK293F cells using PEI (Polysciences). Four days after transfection, the supernatant was collected and filtered through 0.45-μm filter units. The TriTCEs in the supernatant were purified through nickel chromatography (GE Healthcare) and ANTI-FLAG® M1 Agar Affinity Gel (Millipore Sigma). The purified products were analysed by SDS-PAGE under denaturing conditions after deglycosylated by PNGase F (Sigma-Aldrich) to identify the fraction that contained chains as designed. The purified TriTCEs were then aliquoted and kept at − 80 °C for long-term storage.

2.3. Affinity and specificity assay

The binding affinity and specificity of logic-gated dual tumor-targeted TriTCEs to pHLA were tested *via* ELISA. Briefly, 96-well EIA/RIA plates (Corning Incorporated) were coated with streptavidin (2 μg/mL) overnight at 4 ℃. After blocking, different biotin-labelled pHLAs (2 μg/mL), generated by refolding as in a previous report [13] were added for 1 h at 37 ℃. Then, increasing amounts of TriTCEs and the controls were added for 1 h at 37 ℃, followed by incubation with HRP-conjugated goat anti-human IgG (H+L) (1:1000 dilution, Beyotime Biotechnology) for 1 h at 37 ℃. The samples finally reacted with the TMB substrate solution and the reaction was stopped by adding 2 M H_2SO_4. The absorbance of the samples at 450 nm was measured using a Model 680 Microplate Reader (Bio-Rad). Washing by PBST was needed between each step.

To test the binding capacity of dual tumor-targeted TriTCEs to CD3 or EGFR, Jurkat cells (expressing human CD3) or PC9 cells (expressing EGFR) were used as target cells by flow cytometry. Briefly, target cells were harvested and incubated with serial dilutions of TriTCEs or the controls for 30 min at 4 ℃. Then the cells were incubated with FITC-conjugated goat anti-human IgG (H+L) (1:200 dilution, Beyotime Biotechnology) for 30 min at 4 ℃. Samples were analysed by an ACEA NovoCyte™ flow cytometer (ACEA Biosciences). Washing with PBS was needed between each step.

2.4. In vitro cytotoxicity assay

The cytotoxicity of logic-gated dual tumor-targeted TriTCEs was evaluated by apoptosis detection or LDH release assays. PBMCs and target tumor cells were incubated in a 4:1 ratio in the presence of serial dilutions of TriTCEs or the controls. For apoptosis (constructed cell lines that carry GFP), mixed cells were generally incubated in 48-well plates in RPMI-1640 with 10% FBS. After 2 days, samples were harvested and stained using an Annexin V, 633 Apoptosis Detection Kit (Dojindo) and analysed by an ACEA NovoCyte™ flow cytometer. For LDH, mixed cells were generally incubated in 96-well plates in RPMI-1640 (without phenol red) with 1.5% FBS. After 2 days, the supernatants were transferred into new 96 well plates. Following the steps of the LDH Cytotoxicity Assay Kit (Beyotime Biotechnology), the released LDH was represented by the absorbance at 490 nm. The highest absorbance in all samples was regarded as 100%. Each sample was made with three repeats.

2.5. Fluorescence resonance energy transfer (FRET) assay

HEK293T cells were used in the FRET assay to determine the proximity of SLL/A2 (pHLA) and EGFR on tumor cells when tNY-aCD3/aEGFR engaged PBMCs against the tumor cell. Briefly, a plasmid expressing CFP fused with EGFR and a plasmid expressing YFP fused with SLL/A2-YFP were co-transfected into HEK293T cells. At 12 h post-transfection, 3×10^4 cells were transferred into a confocal dish. After another 12 h of incubation, 1.2×10^5 PBMCs with tNY-aCD3/aEGFR or its controls were added into the dish and incubated for 18 h. After

incubation, the fluorescence of the samples at 470 nm and 530 nm was measured in the same field of view by an Olympus high-resolution confocal microscope (60 ×). The ratio of the fluorescence intensity of YFP emission (530 nm) to the fluorescence intensity of CFP emission (470 nm) was used as the evaluation index of the FRET reaction.

2.6. T cell activation, proliferation and cytokine analysis

To identify the active state of T cells in PBMCs under culture conditions as the *in vitro* cytotoxicity assay showed, assays were performed on T cell activation, proliferation, and cytokine production.

For T cell activation, the early activation marker CD69 and late activation marker CD25 on the surface were evaluated by flow cytometry. Briefly, cells were harvested after 2 days of coculture and stained with the following antibodies: Super Bright 436 anti-human CD69 (Invitrogen), PE anti-human CD25 (Invitrogen), and APC anti-human CD3 (Invitrogen), or APC anti-human CD8 (Invitrogen) or APC anti-human CD4 (Invitrogen). Samples were analysed by an ACEA NovoCyte™ flow cytometer.

For T cell proliferation, PBMCs were labeled with CFSE (Invitrogen) according to the manufacturer's protocol before coculture. After 3–8 days of coculture, the cells were harvested, stained with PI (Invitrogen), and analysed by an ACEA NovoCyte™ flow cytometer.

For cytokine analysis, after 2–3 days of coculture, cells and supernatants were collected. Cytokines such as IFN-γ and IL-2 in the supernatant were measured with an IFN gamma Human Uncoated ELISA Kit (Invitrogen) and Human IL-2 Precoated ELISA kit (Dakewe) as described in the instructions. For intracellular granzyme B, cells were fixed and permeabilized by the eBioscience™ Intracellular Fixation & Permeabilization Buffer Set (Invitrogen) as indicated by the manufacturer. Finally, the samples were analysed by an ACEA NovoCyte™ flow cytometer.

2.7. In vivo distribution

To visualize the *in vivo* distribution of logic-gated dual tumor-targeted TriTCE, Cy5 was conjugated to tNY-aCD3/aEGFR or tNY-aCD3/aCtrl *via* sortase A-mediated transpeptidation and click reaction as previously reported [14]. Briefly, 6–8 weeks old female BALB/c Nude mice (GemPharmatech) were intraperitoneally injected with cyclophosphamide once a day at a dose of 50 mg/kg for two days to further inhibit natural immunity and humoral immunity to increase the success rate of tumor transplantation. Then, approximately 5×10^6 A375-SLL$_{high}$ cells or 4×10^6 PC9-SLL cells were inoculated subcutaneously into the right flanks of nude mice. A month after inoculation, mice were intravenously injected with 5×10^6 PBMCs and tNY-aCD3/aEGFR-Cy5 or tNY-aCD3/aCtrl-Cy5 at a dose of 3 mg/kg. The distribution of Cy5 fluorescence in mice was imaged using a Maestro *in vivo* imaging system at different time points after administration. The fluorescence intensity of Cy5 in tumors and background areas (weakest fluorescence) was quantified by CRi Maestro Image software to calculate the tumor/background ratio (TBR). After the last time point, the mice were euthanized by cervical dislocation, and the tissue organs were imaged.

All animal experiments in this paper were performed in accordance with the National Institute of Health Guide for the Care and Use of Laboratory Animals. The protocols were approved by the Committee on the Ethics of Animal Experiments of Zhejiang University, China (ZJU20190536).

2.8. T cell infiltration

6–8 weeks old female BALB/c Nude mice were pretreated with cyclophosphamide as described above. 2.7×10^6 PC9-SLL cells were inoculated subcutaneously into the right flanks of nude mice on day 0, and the mice were randomly divided into 3 groups (3 mice per group): PBS, tNY-aCD3/aEGFR and tNY-aCD3/aCtrl. PBMCs were intravenously injected into mice at 7.5×10^6 per mouse on day 11 and 4.5×10^6 per mouse on day 18, respectively. Each group was intravenously administrated a dose of 2.2 mg/kg on days 11, 14, and 18. Mice were euthanized on day 31, and tumors were resected. Sections were stained with hematoxylin and eosin according to standard protocols or processed for immunohistochemistry [15].

2.9. In vivo antitumor activity

We selected severely immunodeficient mice to compensate for the effect of PBMC on the success rate of tumor transplantation. Briefly, 6–8 weeks old female SCID-Beige mice (GemPharmatech) were subcutaneously co-engrafted with 2×10^6 tumor cells and 2×10^6 PBMCs in the right armpit on day 1, and randomly divided into 4 groups (4 mice per group): saline, tNY-aCD3/aEGFR, tNY-aCD3/aCtrl and tCtrl-aCD3/aEGFR. Each group was intravenously administrated a dose of 100 μg/kg on days 1, 4, and 7. The tumor volume was monitored and recorded according to the following formula: Volume = (Length × Width^2)/2. Mice were euthanized when the tumor volume was larger than 500 mm^3.

2.10. Statistical analysis

Statistical analysis was performed using a two-sided unpaired Student's t-test. A *P*-value less than 0.05 was considered statistically significant. The results were presented as the mean ± S.D.

3. Results

3.1. Logic-gated dual tumor-targeted TriTCE showed high tumor selective and potent antitumor activity in vitro

We selected EGFR (the most commonly targeted TAA) and pHLA (peptide fragments from intracellular proteins presented on the cell surface by human leukocyte antigens) as the tumor targets. Due to the co-expression of NY-ESO-1 and EGFR in various cancer patients (Table S1), we began our study by designing tNY-aCD3/aEGFR (Fig. 1A) to target the HLA-A* 02:01-presented NY-ESO-1 peptide (SLLMWITQC, SLL/A2) and EGFR on tumor cells, and huCD3ε on T cells. Variable domain sequences of 1G4113 (a T cell receptor (TCR) targeting SLL/A2, called tNY here) [16], cetuximab (aEGFR) [17], and HXR32 (aCD3) [18] were used in tNY-aCD3/aEGFR. The isotype controls of tNY-aCD3/aEGFR were engineered by replacing aEGFR with an irrelevant antibody targeting Claudin18.2 (tNY-aCD3/aCtrl) [19], replacing tNY with an irrelevant TCR targeting HLA-A* 02:01-presented TP53 peptide (tCtrl-aCD3/aEGFR) [20], or deleting aCD3 (tNY/aEGFR). Heterodimeric Fc was assembled through the knob-into-hole method [21], and L234A-L235A-P329G mutations in Fc were introduced to eliminate unwanted FcγR-mediated immune effector functions [22]. tNY-aCD3/aEGFR and its controls were successfully produced using standard mammalian expression and affinity purification (Fig. S1A, Table S2). Then, we evaluated the binding activity of tNY-aCD3/aEGFR and its controls using SLL/A2 protein, PC9 (EGFR$^+$), and Jurkat (CD3ε$^+$). As expected, tNY displayed similar affinity and specificity against SLL/A2 here (Fig. S1B and C), and TriTCE with aEGFR or aCD3 exhibited a similar affinity for PC9 cells (Fig. S1D) or Jurkat cells (Fig. S1E). While the controls without tNY, aEGFR, or aCD3 lost the ability to recognize SLL/A2, PC9 cells, or Jurkat cells, respectively.

To evaluate the potency of tNY-aCD3/aEGFR, we performed *in vitro* cytotoxicity assays in which tNY-aCD3/aEGFR and its controls engaged peripheral blood mononuclear cells (PBMCs) against A375-SLL$_{high}$ cells (SLL/A2$^+$, EGFR$^+$, Table S3, Fig. 1 B-C, and S2A, Video). tNY-aCD3/aEGFR (EC_{50} ≈18 pM) showed potent antitumor activity against A375-SLL$_{high}$ cells, while the potency of tNY-aCD3/aCtrl (EC_{50} ≈1300 pM, ~70-fold) and tCtrl-aCD3/aEGFR (EC_{50} ≈13400 pM, ~750-fold)

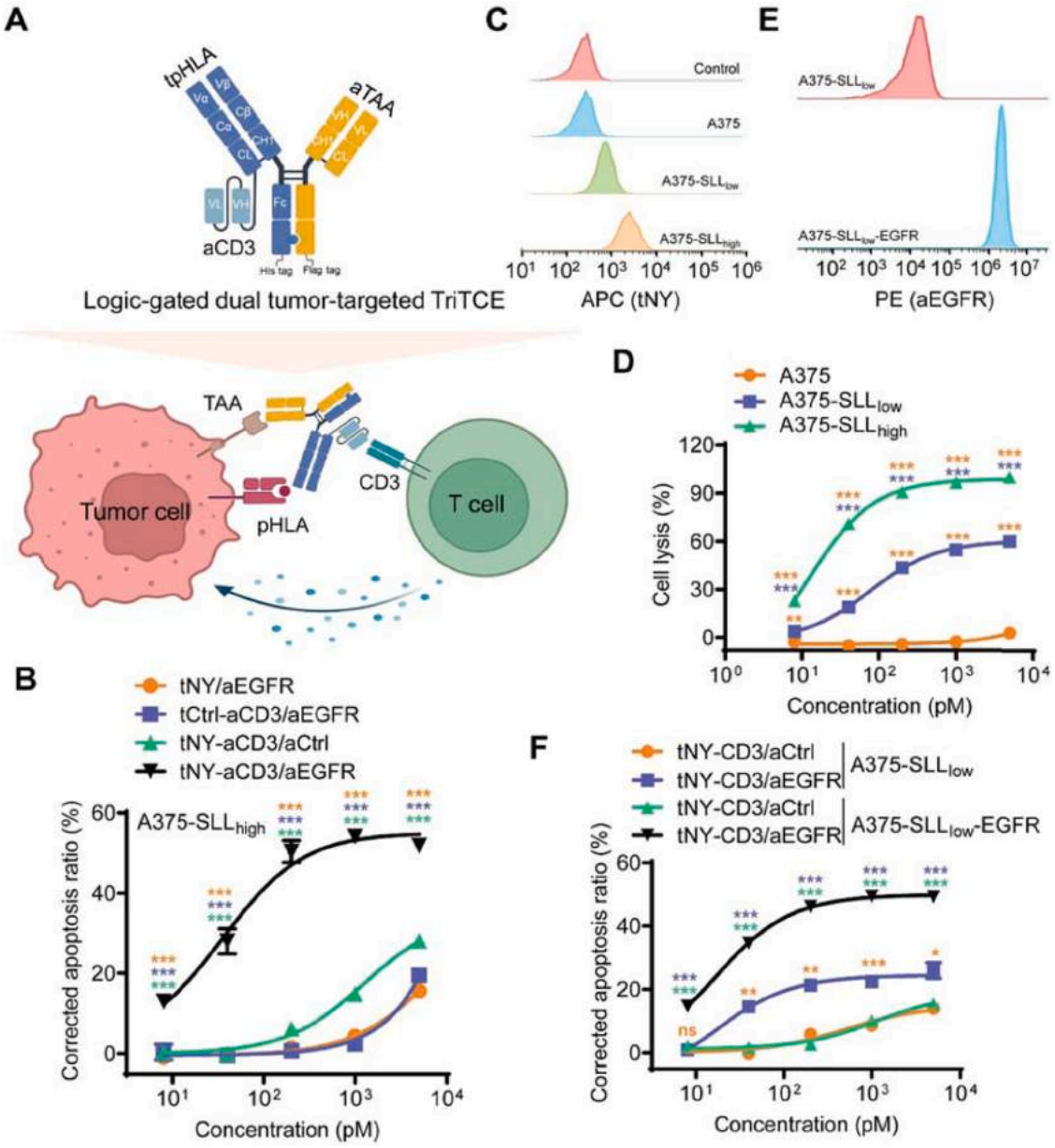

Fig. 1. Design and *in vitro* antitumor activity of the logic-gated dual tumor-targeted TriTCE. (A) The configuration of the logic-gated dual tumor-targeted TriTCEs. The TriTCEs were designed with an optimized spatial configuration to redirect T cells to kill tumor cells after binding pHLA by TCR and EGFR by antibody simultaneously on the same tumor cell. (B) T cell-dependent cytotoxicity of tNY-aCD3/aEGFR and its controls on A375-SLL$_{high}$ cells. A375-SLL$_{high}$ cells were the A375 cells stably transfected with SLLMWITQC peptide and eGFP. The cytotoxicity was indicated by the degree of A375-SLL$_{high}$ cell apoptosis. Apoptotic tumor cells were labeled with Annexin V-633 and PI, and then detected by flow cytometry (n = 3). (C) SLL/A2 expression levels on the surface of A375, A375-SLL$_{high}$ and A375-SLL$_{low}$. After incubation with the tNY-aCD3/aCtrl, the cells were stained with APC-labeled anti-human IgG antibody, and the fluorescence intensity of APC on the cells was compared by flow cytometry. A375-SLL$_{low}$ cells were the A375 cells stably transfected with SLLMWITQC peptide and eGFP. (D) tNY-aCD3/aEGFR redirected T cells to lysis A375, A375-SLL$_{low}$, and A375-SLL$_{high}$ *in vitro*. The cytotoxicity was indicated by tumor cell lysis, which was determined by LDH released level (n = 3). (E) Comparison of EGFR expression levels on the cell surface of A375-SLL$_{low}$ and A375-SLL$_{low}$-EGFR. A375-SLL$_{low}$-EGFR cells were obtained by stably transfecting EGFR in A375-SLL$_{low}$ cells. After incubation with the cetuximab, the cells were stained with PE-labeled anti-human IgG antibody, and the fluorescence intensity of PE on the cells was compared by flow cytometry. (F) tNY-aCD3/aEGFR or tNY-aCD3/aCtrl redirected PBMCs to lysis A375-SLL$_{low}$ and A375-SLL$_{low}$-EGFR *in vitro*. The cytotoxicity was indicated by the degree of tumor cell apoptosis. Apoptotic tumor cells were labeled with Annexin V-633 and PI, and then detected by flow cytometry (n = 3). The statistical differences are shown next to the data points, and the statistical differences with different groups are color-coded accordingly. ns $\geq$ 0.05, * $P < 0.05$, * * $P < 0.01$, * ** $P < 0.001$.

was significantly reduced by single tumor-targeting of either tumor antigen, suggesting that TriTCE markedly enhanced the tumor selectivity of TCE while maintaining high potency. Similar logic-gated cytotoxicity of tNY-aCD3/aEGFR was also shown by different tumor cells (Table S3, Fig. S2A) and different PBMCs (Fig. S2B). Then, we found that the antitumor activity of tNY-aCD3/aEGFR was affected by the expression level of SLL/A2, and the lack of SLL/A2 resulted in the loss of its activity (Fig. 1C-D, Table S3). Likewise, the expression level of EGFR can also influence the potency of tNY-aCD3/aEGFR, as the efficacy of tNY-aCD3/aEGFR and tNY-aCD3/aCtrl engaged PBMCs against K562-SLL cells (SLL/A2 +, EGFR-, Table S3) was comparable and increasing the expression of EGFR was beneficial to the efficacy of tNY-aCD3/aEGFR (Fig. 1E-F, Table S3).

Supplementary material related to this article can be found online at

doi:10.1016/j.phrs.2023.106781.

In addition, the antitumor activity of tNY-aCD3/aEGFR was more potent than that of the combination of tNY-aCD3/aCtrl and tCtrl-aCD3/aEGFR (aCtrl+tCtrl, Fig. 2A), indicating the high activity of dual antigen-targeted TriTCE was not simply a superposition of the potency of two single antigen-targeted TCEs. To further study the active mechanism of dual antigen-targeted TriTCE, we implemented a FRET assay. After co-incubated with PBMCs and HEK293T-EGFR-SLL/A2 cells (co-expressing EGFR-CFP and SLL/A2-YFP, Fig. 2B), the FRET efficiency of the tNY-aCD3/aEGFR group was significantly higher than that of the control groups (Fig. 2C-D), suggesting that EGFR and SLL/A2 aggregated after simultaneous targeting by TriTCE. Hence, we hypothesized that the spatial proximity of the dual tumor antigens caused by TriTCE might be an important reason for achieving its logic-gated activity.

3.2. *tNY-aCD3/aEGFR efficiently activated T cells to proliferate and release cytokines*

We next assayed tNY-aCD3/aEGFR and its controls for their ability to activate T cells *in vitro*. As shown in Fig. 3A, tNY-aCD3/aEGFR significantly increased CD69 (early marker) and CD25 (intermediate or late marker) expression in T cells in a dose-dependent manner and more efficiently than its controls when PBMCs were co-cultured with A375-SLL_{high} cells for 48 h. The T cell activation assay after treatment with

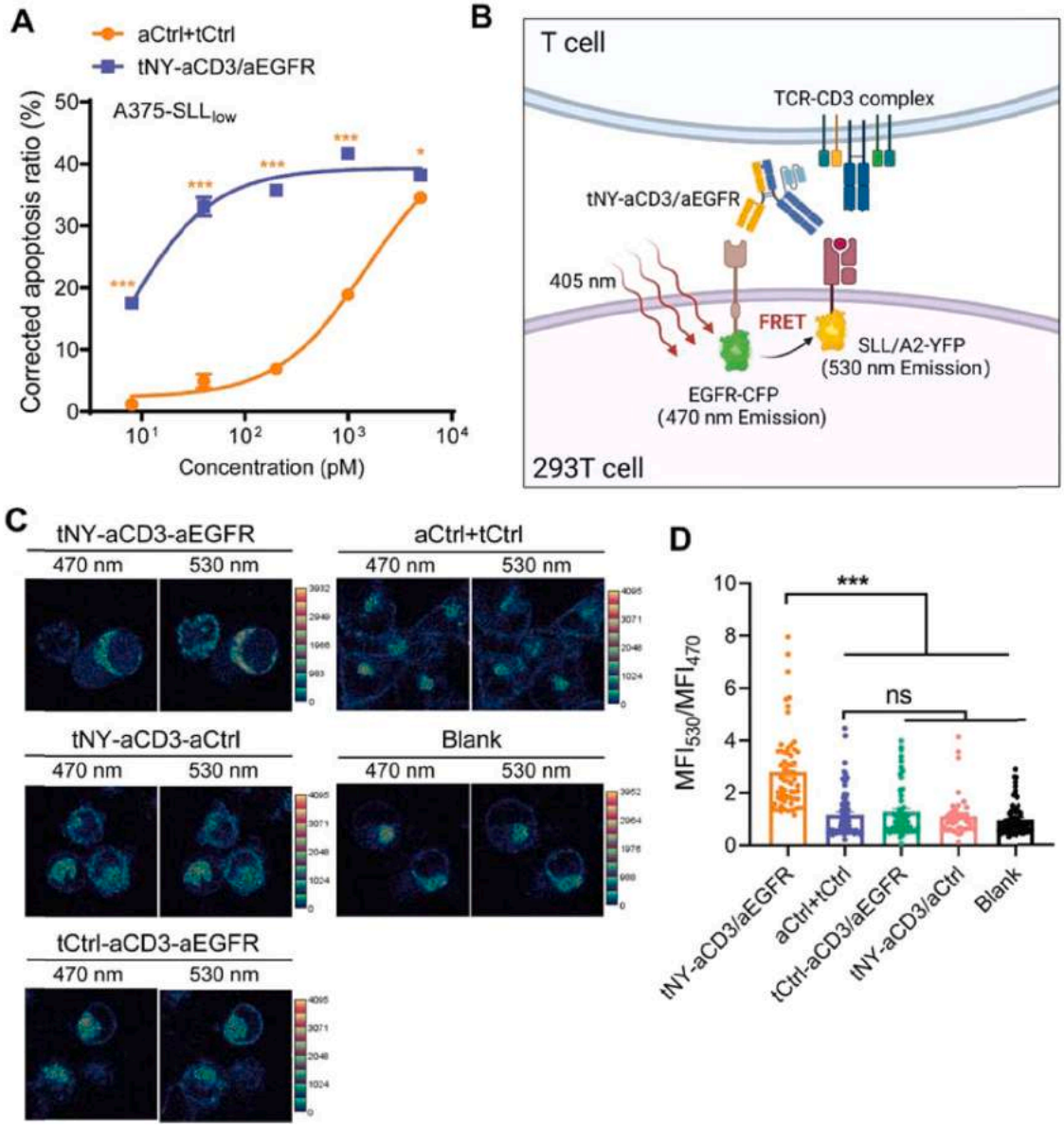

Fig. 2. Mechanism of the T cell-dependent cytotoxicity of tNY-aCD3/aEGFR. (A) T cell-dependent cytotoxicity of tNY-aCD3/aEGFR or combination with tNY-aCD3/aCtrl and tCtrl-aCD3/aEGFR (aCtrl+tCtrl) on A375-SLL_{low} cells. The cytotoxicity was indicated by the degree of A375-SLL_{low} cell apoptosis. Apoptotic tumor cells were labeled with Annexin V-633 and PI, and then detected by flow cytometry (n = 3). (B) Schematic diagram of FRET reaction induced by antigen aggregation. CFP and YFP are fused to the carboxyl terminus of EGFR and SLL/A2, respectively. When induced by the tNY-aCD3/aEGFR and T cells, EGFR and SLL/A2 were aggregated (<10 nm), resulting in the emission of light (~470 nm) from CFP being absorbed by YFP to emit light of about 530 nm. (C) Proximity-induced FRET assay after treatment with tNY-aCD3/aEGFR, tNY-aCD3/aCtrl, tCtrl-aCD3/aEGFR or aCtrl+tCtrl on HEK293 T-EGFR-SLL/A2 cells. The stronger the light of 530 nm and the weaker the light of 470 nm, the stronger the FRET reaction, *i.e.*, the higher the aggregation degree of EGFR and SLL/A2. (D) FRET efficiency between EGFR-CFP and SLL/A2-YFP after treatment with tNY-aCD3/aEGFR, tNY-aCD3/aCtrl, tCtrl-aCD3/aEGFR or aCtrl+tCtrl on HEK293 T-EGFR-SLL/A2 cells. Over 43 regions of cell members from different cells were examined by the FRET study. The statistical differences are shown next to the data points, and the statistical differences with different groups are color-coded accordingly. ns ≥ 0.05, $^{*}P < 0.05$, $^{**}P < 0.01$, $^{***}P < 0.001$.

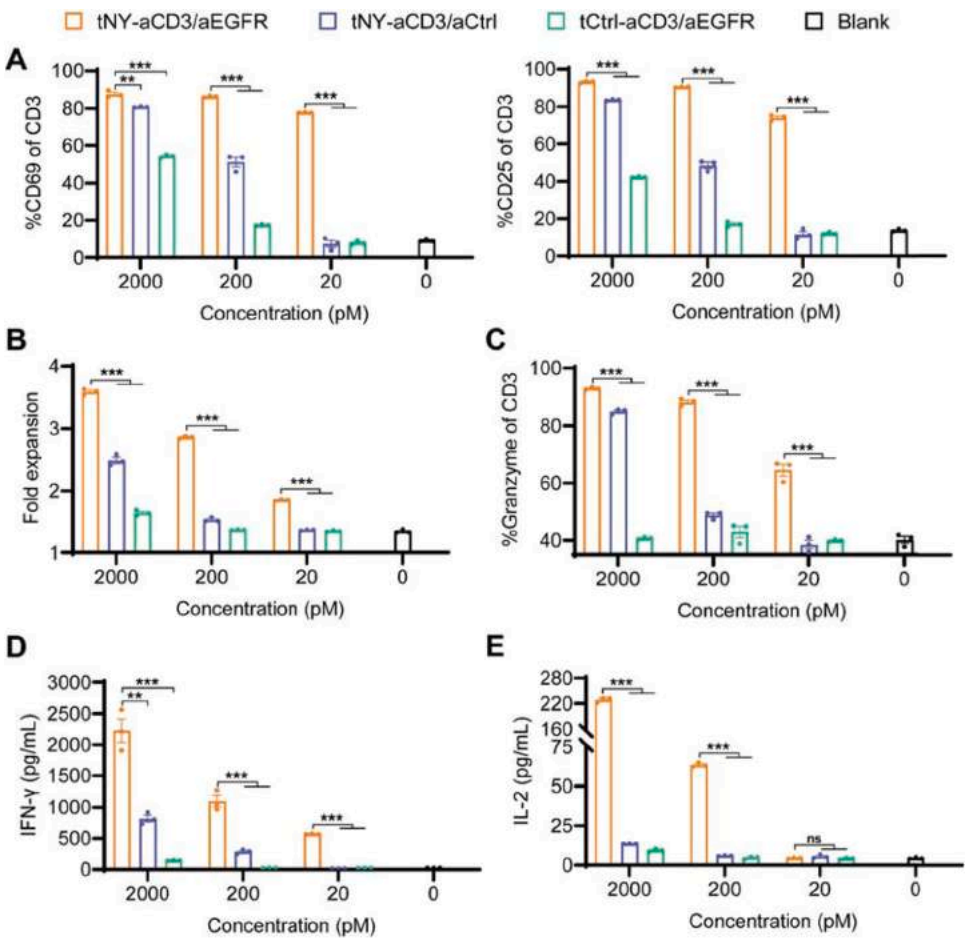

Fig. 3. T cell activation, proliferation, and cytokines release in response to the stimulation of tNY-aCD3/aEGFR or its controls. (A) T cell activation mediated by tNY-aCD3/aEGFR or its controls in the presence of A375-SLL$_{high}$ cells for 48 h was marked as CD69 or CD25 positive (n = 3). (B) Mean fold expansion of T cells mediated by tNY-aCD3/aEGFR or its controls in the presence of A375-SLL$_{high}$ cells for 96 h (n = 3). (C) Up-regulation of granzyme B^{+} T cell ratio mediated by tNY-aCD3/aEGFR or its controls in the presence of A375-SLL$_{high}$ cells for 48 h (n = 3). (D-E) IFN-γ (D) and IL-2 (E) release of PBMCs mediated by tNY-aCD3/aEGFR or its controls in the presence of A375-SLL$_{high}$ cells for 72 h (n = 3). ns $\geq$ 0.05, *P < 0.05, **P < 0.01, ***P < 0.001.

tNY-aCD3/aEGFR or its controls for 72 h (Fig. S3A) was similar to that at 48 h, indicating that T cell activation may have approached its peak at 48 h. While T cells specifically proliferated after incubation with tNY-aCD3/aEGFR and A375-SLL$_{high}$ cells for 72 h (Fig. S3B) and 96 h (Figs. 3B and S3C). In fact, the proliferation of T cells increased significantly and continuously within 148 h (Fig. S3D-E), which was beneficial for T cells to execute tumor-killing activity lastingly. Furthermore, the mean expansion fold of T cells was decreased after 192 h, hinting at the onset of T cell exhaustion (Fig. S3D-E).

To further assess the antitumor activity of activated T cells, we performed a granzyme B expression and cytokine release assays. Granzyme B-positive T cells were up-regulated in a time- and dose-dependent manner (Fig. S4A) after co-incubation with tNY-aCD3/aEGFR and A375-SLL$_{high}$ cells, and granzyme B was delivered to A375-SLL$_{high}$ cells (Fig. S4B) to exert antitumor activity. Compared with tNY-aCD3/aCtrl and tCtrl-aCD3/aEGFR, tNY-aCD3/aEGFR significantly activated T cells to express (Fig. 3C) and deliver (Fig. S4C) granzyme B, suggesting that the activation was logically gated. In addition, tNY-aCD3/aEGFR can activate T cells to release a large amount of IFN-γ (Fig. 3D) and IL-2 (Fig. 3E) more effectively than the controls, which was consistent with the antitumor activity results and further provided evidence for the logic-gated antitumor activity of tNY-aCD3/aEGFR.

3.3. *tNY-aCD3/aEGFR can effectively enrich in the tumor site and execute its antitumor activity in vivo*

To determine the tumor-targeting ability of tNY-aCD3/aEGFR *in vivo*, we observed the distribution of tNY-aCD3/aEGFR in two xenograft models (A375-SLL$_{high}$ and PC9-SLL). The fluorescence intensity of tumor tissue in A375-SLL$_{high}$ (Figs. 4A-B and S5A) and PC9-SLL (Fig. S5A-C) xenograft mice were significantly enhanced at 18 h after tail vein injection of tNY-aCD3/aEGFR-Cy5, and the fluorescence remained in the tumors for at least 45 h, indicating that tNY-aCD3/aEGFR massively accumulated in tumor sites. Although the fluorescence intensity of the tumor tissue slightly increased after being injected with tNY-aCD3/aCtrl-Cy5, it was generally much weaker than that in tNY-aCD3/aEGFR-Cy5 treated xenograft mice, especially with a significant difference at approximately 2–3 days (Figs. 4A-B and S5B-C). Therefore, dual tumor-targeting may also facilitate the aggregation of TriTCE at the tumor site, thereby further enhancing its anti-tumor activity.

In order to assess the ability of tNY-aCD3/aEGFR to promote immune infiltration, we injected PBMCs and tNY-aCD3/aEGFR or its controls into PC9-SLL xenografted mice *via* the tail vein, and then analysed resected tumors using immunohistochemistry. The numbers of infiltrating T cells were generally higher in tNY-aCD3/aEGFR-treated mice than in PBS or tNY-aCD3/aCtrl-treated mice (Fig. 4C-D).

To further study the therapeutic effect of tNY-aCD3/aEGFR *in vivo*, we co-inoculated A375-SLL$_{high}$ cells and PBMCs subcutaneously into SCID-Beige mice, and then treated them with tNY-aCD3/aEGFR or its controls through the tail vein on days 1, 4, and 7. The ability of tNY-aCD3/aEGFR to inhibit tumor growth (Figs. 5A and S5D) and prolong the survival time of mice (Fig. 5B) was significantly greater than that of the controls, indicating the specific *in vivo* antitumor activity of tNY-aCD3/aEGFR. Moreover, tNY-aCD3/aEGFR also showed specific antitumor activity in the A375-SLL$_{low}$-EGFR xenograft mouse model (Figs. 5C-D and S5E).

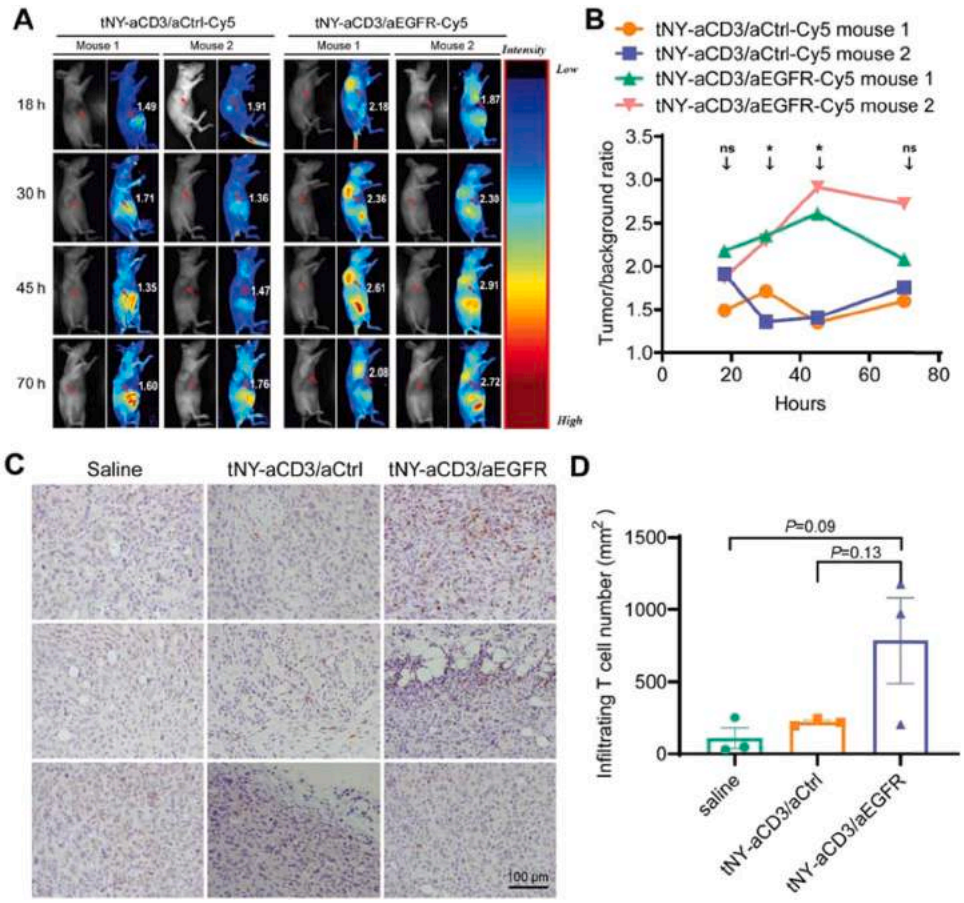

Fig. 4. The ability of tNY-aCD3/aEGFR to enrich and mediate T cell infiltration in solid tumors. (A-B) *In vivo* distribution of tNY-aCD3/aEGFR-Cy5 or tNY-aCD3/aCtrl-Cy5 in A375-SLL_{high} burdened mice. The distribution of tNY-aCD3/aEGFR or tNY-aCD3/aCtrl was indicated by the fluorescence intensity of Cy5, which was imaged using a Maestro *in vivo* imaging system at different time points after administration. Tumor locations were designated by red arrows (A). The fluorescence intensity of Cy5 in tumors was presented by tumor/background ratio (TBR), which was shown next to the tumor (A) and made into a line chart to show its trend over time (B). The statistical differences of TBR between tNY-aCD3/aEGFR-Cy5 and tNY-aCD3/aCtrl-Cy5 groups at different time points were shown in corresponding positions (n = 2, B). ns ≥ 0.05, * $P < 0.05$, * * $P < 0.01$, * ** $P < 0.001$. (C-D) T cell infiltration in the tumor tissue of PC9-SLL burdened mice treated with PBMCs and tNY-aCD3/aEGFR or its controls. Typical area of T cell infiltration in tumor (C). According to T cell infiltration density, preliminarily estimated and selected the top 5 areas (~0.2 mm × 0.2 mm) of T cell infiltration to manually count the number of infiltrated T cells, and converted it into the number of infiltrated T cells per square millimetre (D).

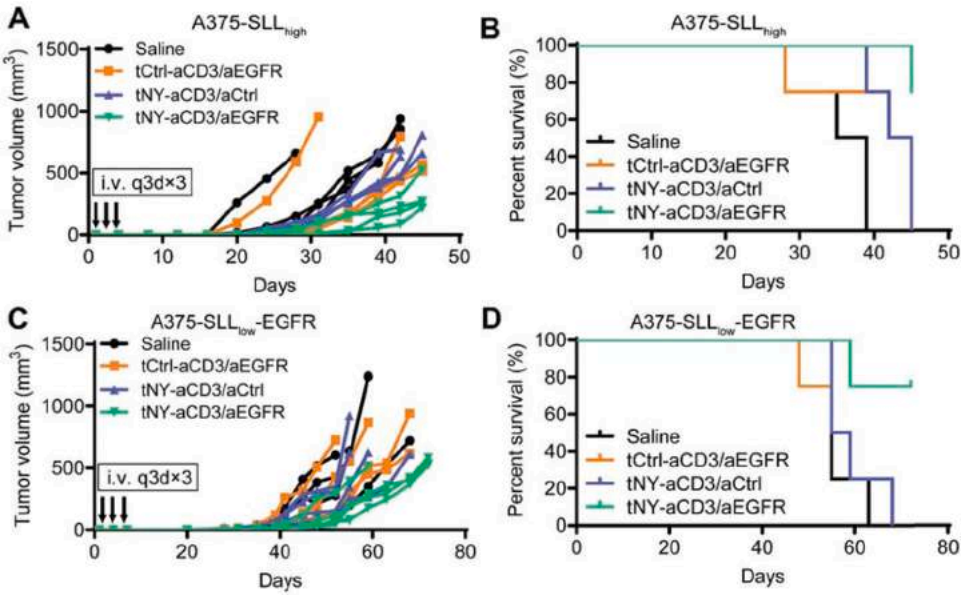

Fig. 5. *In vivo* efficacy of tNY-aCD3/aEGFR and its controls in mouse xenograft model. (A, C) Tumor volume of A375-SLL_{high} (A) or A375-SLL_{low}-EGFR (C) xenograft model at different time points. (B, D) Survival rate of the A375-SLL_{high} (B) or A375-SLL_{low}-EGFR (D) xenograft model mice. Mice with a tumor volume greater than 500 mm^3 were judged to be dead. SCID-Beige mice engrafted with tumor cells (2×10^6) and PBMCs (2×10^6) were treated with saline or 100 μg/kg drugs intravenously at days 1, 4, and 7 (n = 4).

3.4. The concept of logic-gated dual tumor-targeted TriTCE was applied to different targets

Finally, we confirmed whether the logic-gated dual tumor-targeted TriTCE was applicable to different targets. We selected the TCR-mimic antibody (TCRm) variable domain sequences of ESK1 (aWT1) [23], which targeted the HLA-A* 02:01 presented-WT1 peptide (RMFPNAPYL, RMF/A2), and then prepared aWT1-aCD3/aEGFR and its control (aWT1-aCD3/aCtrl) (Figs. 6A and S6A, Table S4). aWT1-aCD3/aEGFR showed specific affinity for RMF/A2, EGFR and CD3, while the controls lost the corresponding affinity (Fig. S6B-E). The ability of aWT1-aCD3/aEGFR engaged PBMCs against BV173-EGFR cells (SLL/$A2^+$, $EGFR^+$, Table S5) was much greater than that of the controls (Fig. 6B), indicating the logic-gated antitumor activity of

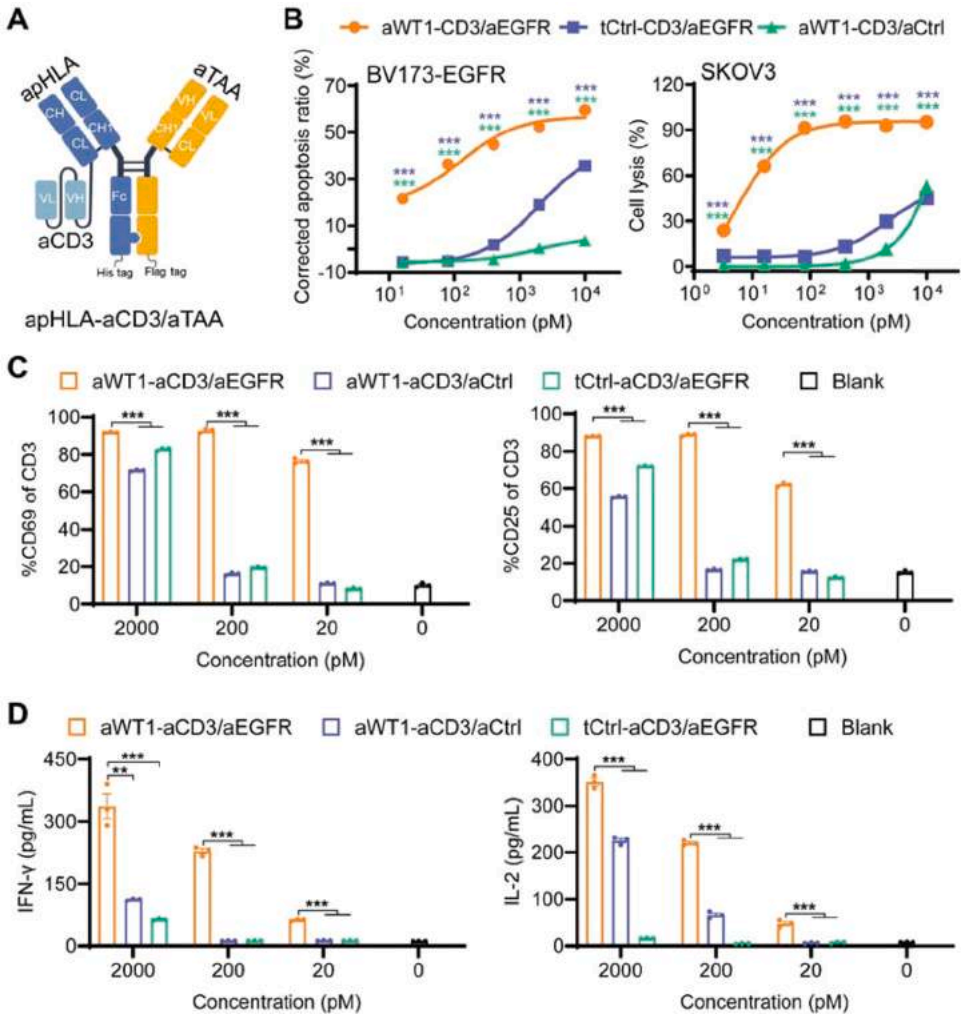

Fig. 6. Specific tumor cytotoxicity and T cell activation elicited by aWT1-aCD3/aEGFR. (A) The schematic diagram of aWT1-aCD3/aEGFR. The aWT1-aCD3/aEGFR was designed with two antibodies that target pHLA (apHLA) and TAA (aTAA), respectively. (B) T cell-dependent cytotoxicity of aWT1-aCD3/aEGFR and its controls on BV173-EGFR cells and SKOV3 cells. BV173-EGFR cells were the BV173 cells stably transduced with EGFR and eGFP. The cytotoxicity was indicated by the degree of BV173-EGFR cell apoptosis or SKOV3 cell lysis. Apoptotic tumor cells were labeled with Annexin V-633 and PI, and then detected by flow cytometry (n = 3). Cell lysis was determined by LDH released level (n = 3). (C) T cell activation mediated by aWT1-aCD3/aEGFR or its controls in the presence of SKOV3 cells for 48 h (n = 3). (D) IFN-γ and IL-2 secretion of PBMCs mediated by aWT1-aCD3/aEGFR or its controls in the presence of SKOV3 cells for 72 h (n = 3). ns ≥ 0.05, * $P < 0.05$, * * $P < 0.01$, * ** $P < 0.001$.

aWT1-aCD3/aEGFR, which was consistent with the T cell-dependent cytotoxicity of tNY-aCD3/aEGFR. The higher antitumor activity of aWT1-aCD3/aEGFR against BV173-EGFR cells compared with BV173 cells (RMF/A2$^+$, EGFR$^-$ Table S5) also showed that targeting dual tumor targets can indeed improve the antitumor activity of TriTCE (Fig. S7). Surprisingly, aWT1-aCD3/aEGFR can specifically mediate PBMCs to lyse SKOV3 cells (native RMF/A2 and EGFR positive cells, Table S5), suggesting the potential therapeutic value of aWT1-aCD3/aEGFR (Fig. 6B), which was further evidence that the concept of logic-gated dual tumor-targeted TriTCE has potential applications. As expected, T cell activation (Fig. 6C) and cytokine release (Fig. 6D) were obviously observed after treatment with different concentrations of aWT1-aCD3/aEGFR, while the controls induced T cell activation and cytokine release only at high concentrations. That is to say, the concept of logic-gated dual tumor-targeted TriTCE has a certain universality.

4. Discussion

TCEs have demonstrated their therapeutic potential in the clinic [1], while improving the efficacy and selectivity of TCEs for tumors, especially solid tumors [4], is still required. Here, we report a novel type of dual tumor-targeted TriTCEs, designed to retarget T cells toward cancer cells more effectively and specifically.

Commonly used antigens in tumor therapies (*e.g.*, HER2 and EGFR) are often expressed in some normal cells, and targeting these antigens may cause on-target off-tumor toxicity [24,25]. It is worth noting that different tumor antigens are not necessarily expressed in the same normal cells/tissues. Therefore, triggering the activity of TCE by multiple tumor antigens can theoretically effectively reduce on-target off-tumor toxicity. Due to the co-expression of NY-ESO-1 and EGFR in tumor cells, and the main expression of NY-ESO-1 in non-survival requirement organs such as the testis and placenta [26,27], we chose these two antigens to design TriTCE (tNY-aCD3/aEGFR). We found that dual-tumor targeting was crucial for the function of TriTCE, but it had poor activity against NY-ESO-1 and EGFR positive A375 cells. NY-ESO-1 is a cytoplasmic protein that is difficult to directly target by macromolecular drugs such as TCEs. SLL/A2, a pHLA generated from an NY-ESO-1 derived peptide bound to human leucocyte antigen (HLA), is the true target of tNY-aCD3/aEGFR [26], and its expression level is extremely low (no more than 50 copies per cell) [28] to detect by flow cytometry. We therefore proposed that an appropriate antigen expression level rather than the tumor specificity of the antigen is more important for TriTCEs. As another example, RMF/A2 (which can be detected by flow cytometry)-targeted TriTCE showed robust activity against BV173-EGFR and SKOV3 cells while maintaining its high tumor selectivity, although WT1 (RMF/A2 generated from WT1 derived peptide) had far less tumor specificity than NY-ESO-1 [29,30]. In addition, the absence or insufficient expression of EGFR also sharply reduced the activity of TriTCE, indicating that both tumor antigens contributed significantly to TriTCE activity. Moreover, regulating the expression of any antigen can significantly affect TriTCE activity, and this evidence points to the same fact that TriTCE is truly logic-gated by dual tumor antigens. However, the contribution of the two tumor antigens to TriTCE activity is uneven, and the cis-configuration between CD3 and the tumor antigen binding

domain was more prominent. Hence, changing the configuration of the tumor antigen and CD3 binding domains may affect the activity and specificity of TriTCE.

Unfortunately, the two dual-antigen combinations we have chosen are not commonly used in clinical settings. Although NY-ESO-1 and EGFR are highly co-expressed in some tumor cells, SLL/A2 expression is often extremely low to achieve logic-gated activity for TriTCE. We found in previous studies that NY-ESO-1 is difficult to degrade to generate the SLLMWITQC peptide, thereby limiting the expression of SLL/A2 [31]. Directly increasing the content of SLLMWITQC peptides in tumor cells can effectively improve the expression of SLL/A2 [31], but this is difficult to achieve in clinical applications. For aWT1-aCD3/aEGFR, the expression level of RMF/A2 is sufficient to support logic-gated activity, but the co-expression of WT1 and EGFR is not very common. Considering the limited impact on the safety of TriTCE caused by the tumor specificity of a single antigen, we believe that paired antigens with relatively high expression levels that are not co-expressed in healthy cells or only co-expressed in non-survival requirement organs may be more applicable for TriTCE design.

Preliminary mechanistic studies demonstrated that the spatial proximity of the dual tumor antigens was crucial for the potent anti-tumor activity of TriTCEs. As the clustering of pHLA (tumor antigens) is important for optimal T cell responses [32–34], we supposed that inducing antigen aggregation at the cell-cell interface was the intrinsic factor determining the logic gated activity of dual tumor-targeted TriTCEs, which cannot be achieved by single tumor targeted TCEs. However, the expression level of SLL/A2 might be too low to induce antigen aggregation, leading to the suboptimal activity of TriTCE against A375 cells. In addition, some antigens inherently interact or aggregate at the tumor cell surface (*e.g.*, HER3 & EGFR or HER3 & HER2) [35,36], which we believe can be synergistic with TriTCE-induced antigen aggregation, resulting in greater tumor selectivity and activity. Although we have proven that TCE activity can be improved by antigen aggregation, dual-tumor targeting may not be the only way to induce antigen aggregation. Some studies have shown that bivalent tumor targeting arms are beneficial for TCE activity [12,37], so we speculated that bivalent binding to the same tumor antigen can also induce antigen aggregation. Therefore, dual WT1 or dual EGFR targeting may also achieve an increase in TCE activity. Nevertheless, dual targeting of the same antigen may not have much effect on controlling on-target off-tumor toxicity.

Another interesting finding is that weak CD3 affinity (MFI <2) is sufficient to support the potent antitumor activity of TriTCE. Although high CD3-binding affinity is beneficial for the activity of TCEs, it also results in enhanced non-specific activation of T cells and large consumption of TCEs by circulating T cells before reaching the tumor tissue, leading to off-target toxicity (*e.g.*, cytokine storm and damage to healthy tissues by extensively activated T cells) [2,38]. We found that the isotype controls of TriTCEs here can only weakly activate T cells at high concentrations, and more surprisingly, EGFR-targeted controls hardly induced T cell proliferation and cytokine secretion in the presence of tumor cells. These results not only further confirmed the dual tumor antigen-gated activity of TriTCEs, but also reminded us of the high safety of TriTCEs from the off-target toxicity perspective. Even more interestingly, the significant difference in T cell activation between TriTCE and its controls suggested that appropriate enhancement of CD3 affinity may further enhance TriTCE activity while maintaining a low degree of non-specific T cell activation. However, the impact of CD3 affinity on TriTCE activity and specificity has not been studied here, and the optimal range of CD3 affinity for TriTCE design still needs further research.

The *in vivo* potency of TriTCE is superior to that of its controls as well. Expectedly, dual-tumor targeting increases the number of TCE-targeted antigens on the tumor surface, leading to more drug aggregation at the tumor site and enhancing T cell infiltration, which provided further assurance for the *in vivo* activity of TriTCE. However, the *in vivo* activity of TriTCE has been studied based on immune reconstructed mouse xenograft models, and there are still some issues that cannot be explained. Firstly, mouse cells do not express human EGFR, SLL/A2, and RMF/A2, so the xenograft models cannot reflect the potential effect of TriTCE in reducing on-target off-tumor toxicity *in vivo*. A single antigen-positive xenograft model can be used as an alternative to explain the effect of dual-tumor targeting on the control of off-tissue toxicity as well, but it was not presented in the study either. Secondly, mice are also unable to continuously provide human T cells, and the content and distribution of T cells in mice after immune reconstitution may differ from the actual situation. CD3 humanized mice can overcome the above problems [39], providing the possibility for a more accurate evaluation of the efficacy and non-specific T cell activation of TriTCE.

5. Conclusion

We designed novel dual tumor-targeted TriTCEs and found that they were dozens to thousands of times more effective than single tumor-targeted isotype controls. Hence, this logic-gated dual tumor-targeting is an effective strategy to improve the tumor selectivity of TCEs. Through mechanistic study, the aggregation of dual antigens was considered to be the key to achieving the logic gated activity of TriTCEs. Moreover, dual tumor-targeting may also facilitate TriTCE aggregation and T cell infiltration at the tumor site, thereby further enhancing the anti-tumor activity of TCEs.

Ethics approval and consent to participate

All animal experiments here were performed in accordance with the National Institute of Health Guide for the Care and Use of Laboratory Animals. The protocols were approved by the Committee on the Ethics of Animal Experiments of the Zhejiang University, China (permit number : ZJU20190536).

Funding

This work was supported by the National Natural Science Foundation of China (U20A20409 and 82204413), the Zhejiang Provincial Natural Science Foundation (LGF22H300014), and the Key Laboratory of Prevention, Diagnosis and Therapy of Upper Gastrointestinal Cancer of Zhejiang Province (2022E10021).

CRediT authorship contribution statement

Ying Shen: Data curation, Formal analysis, Investigation, Methodology, Resources, Visualization, Roles/Writing – original draft, Writing – review & editing. **Shi-jie Jin**: Formal analysis, Investigation, Methodology, Visualization. **Yi-chang Chen**: Formal analysis, Investigation, Methodology. **Wen-hui Liu**: Investigation, Methodology. **Yi-ming Li:** Investigation. **Wen-yi Zhao:** Investigation. **Ying-chun Xu**: Investigation, Resources. **Shu-qing Chen**: Conceptualization, Data curation, Funding acquisition, Project administration, Supervision, Validation, Roles/Writing – original draft, Writing – review & editing. **Wen-bin Zhao**: Conceptualization, Data curation, Formal analysis, Funding acquisition, Investigation, Methodology, Project administration, Resources, Supervision, Validation, Visualization, Roles/Writing – original draft, Writing – review & editing.

Conflict of interest

The authors declare that they have no competing interests.

Data availability

Data will be made available on request.

Acknowledgements

We thank Shuang-shuang Liu from the Core Facilities, Zhejiang University School of Medicine for her laser scanning confocal microscopy technical support.

Consent for publication

Not applicable.

Appendix A. Supporting information

Supplementary data associated with this article can be found in the online version at doi:10.1016/j.phrs.2023.106781.

References

[1] A. Esfandiari, S. Cassidy, R.M. Webster, Bispecific antibodies in oncology, Nat. Rev. Drug Discov. 21 (6) (2022) 411–412.
[2] A.F. Labrijn, M.L. Janmaat, J.M. Reichert, P.W.H.I Parren, Bispecific antibodies: a mechanistic review of the pipeline, Nat. Rev. Drug Discov. 18 (8) (2019) 585–608.
[3] M.E. Goebeler, S. Knop, A. Viardot, P. Kufer, M.S. Topp, H. Einsele, R. Noppeney, G. Hess, S. Kallert, A. Mackensen, K. Rupertus, L. Kanz, M. Libicher, D. Nagorsen, G. Zugmaier, M. Klinger, A. Wolf, B. Dorsch, B.D. Quednau, M. Schmidt, J. Scheele, P.A. Baeuerle, E. Leo, R.C. Bargou, Bispecific T-cell engager (BiTE) antibody construct blinatumomab for the treatment of patients with relapsed/refractory non-hodgkin lymphoma: final results from a phase I study, J. Clin. Oncol. 34 (10) (2016) 1104–1111.
[4] M. de Miguel, P. Umana, A.L. Gomes de Morais, V. Moreno, E. Calvo, T-cell-engaging therapy for solid tumors, Clin. Cancer Res. 27 (6) (2021) 1595–1603.
[5] H. Li, P. Er Saw, E. Song, Challenges and strategies for next-generation bispecific antibody-based antitumor therapeutics, Cell Mol. Immunol. 17 (5) (2020) 451–461.
[6] Z. Tian, M. Liu, Y. Zhang, X. Wang, Bispecific T cell engagers: an emerging therapy for management of hematologic malignancies, J. Hematol. Oncol. 14 (1) (2021) 75.
[7] Y. Wu, M. Yi, S. Zhu, H. Wang, K. Wu, Recent advances and challenges of bispecific antibodies in solid tumors, Exp. Hematol. Oncol. 10 (1) (2021) 56.
[8] S.C. Oostindie, D.A. Rinaldi, G.G. Zom, M.J. Wester, D. Paulet, K. Al-Tamimi, E. van der Meijden, J.R. Scheick, T. Wilpshaar, B. de Jong, M. Hoff-van den Broek, R.M. Grattan, J.J. Oosterhoff, J. Vignau, S. Verploegen, P. Boross, F.J. Beurskens, D.S. Lidke, J. Schuurman, R.N. de Jong, Logic-gated antibody pairs that selectively act on cells co-expressing two antigens, Nat. Biotechnol. 40 (10) (2022) 1509–1519.
[9] A. Banaszek, T.G.P. Bumm, B. Nowotny, M. Geis, K. Jacob, M. Wölfl, J. Trebing, K. Kucka, D. Kouhestani, T. Gogishvili, B. Krenz, J. Lutz, L. Rasche, D. Hönemann, H. Neuweiler, J.C. Heiby, R.C. Bargou, H. Wajant, H. Einsele, G. Riethmüller, G. Stuhler, On-target restoration of a split T cell-engaging antibody for precision immunotherapy, Nat. Commun. 10 (1) (2019) 5387.
[10] A. Tapia-Galisteo, Í. Sánchez Rodríguez, O. Aguilar-Sopeña, S.L. Harwood, J. Narbona, M. Ferreras Gutierrez, R. Navarro, L. Martín-García, C. Corbacho, M. Compte, J. Lacadena, F.J. Blanco, P. Chames, P. Roda-Navarro, L. Álvarez-Vallina, L. Sanz, Trispecific T-cell engagers for dual tumor-targeting of colorectal cancer, Oncoimmunology 11 (1) (2022) 2034355.
[11] D.M. Dicara, S. Bhakta, J. Go, M.A. Ziai, R. Firestein, B. Forrest, C. Gu, S.R. Leong, G. Lee, S.F. Yu, A.G. Polson, N.J. Agard, Development of T-cell engagers selective for cells co-expressing two antigens, MAbs 14 (1) (2022) 2115213.
[12] B.H. Santich, J.A. Park, H. Tran, H.F. Guo, M. Huse, N.V. Cheung, Interdomain spacing and spatial configuration drive the potency of IgG-[L]-scFv T cell bispecific antibodies, Sci. Transl. Med. 12 (534) (2020), eaax1315.
[13] G. Denkberg, C.J. Cohen, D. Segal, A.F. Kirkin, Y. Reiter, Recombinant human single-chain MHC-peptide complexes made from *E. coli* by in vitro refolding: functional single-chain MHC-peptide complexes and tetramers with tumor associated antigens, Eur. J. Immunol. 30 (12) (2000) 3522–3532.
[14] C.X. Qiu, X.F. Bai, Y. Shen, Z. Zhou, L.Q. Pan, Y.C. Xu, W.B. Zhao, S.Q. Chen, Specific inhibition of tumor growth by T cell receptor-drug conjugates targeting intracellular cancer-testis antigen NY-ESO-1/LAGE-1, Bioconjug. Chem. 31 (12) (2020) 2767–2778.
[15] J.A. Ramos-Vara, Principles and methods of immunohistochemistry, Methods Mol. Biol. 2017 (1641) 115–128.
[16] Y. Li, R. Moysey, P.E. Molloy, A.L. Vuidepot, T. Mahon, E. Baston, S. Dunn, N. Liddy, J. Jacob, B.K. Jakobsen, J.M. Boulter, Directed evolution of human T-cell receptors with picomolar affinities by phage display, Nat. Biotechnol. 23 (3) (2005) 349–354.
[17] J. Graham, M. Muhsin, P. Kirkpatrick, Cetuximab, Nat. Rev. Drug Discov. 3 (7) (2004) 549–550.
[18] J. Douglass, E.H. Hsiue, B.J. Mog, M.S. Hwang, S.R. DiNapoli, A.H. Pearlman, M. S. Miller, K.M. Wright, P.A. Azurmendi, Q. Wang, S. Paul, A. Schaefer, A.D. Skora, M.D. Molin, M.F. Konig, Q. Liu, E. Watson, Y. Li, M.B. Murphy, D.M. Pardoll, C. Bettegowda, N. Papadopoulos, S.B. Gabelli, K.W. Kinzler, B. Vogelstein, S. Zhou, Bispecific antibodies targeting mutant RAS neoantigens, Sci. Immunol. 6 (57) (2021) eabd5515.
[19] H. Jiang, Z. Shi, P. Wang, C. Wang, L. Yang, G. Du, H. Zhang, B. Shi, J. Jia, Q. Li, H. Wang, Z. Li, Claudin18.2-specific chimeric antigen receptor engineered T cells for the treatment of gastric cancer, J. Natl. Cancer Inst. 111 (4) (2019) 409–418.
[20] D. Wu, D.T. Gallagher, R. Gowthaman, B.G. Pierce, R.A. Mariuzza, Structural basis for oligoclonal T cell recognition of a shared p53 cancer neoantigen, Nat. Commun. 11 (1) (2020) 2908.
[21] H. Wei, H. Cai, Y. Jin, P. Wang, Q. Zhang, Y. Lin, W. Wang, J. Cheng, N. Zeng, T. Xu, A. Zhou, Structural basis of a novel heterodimeric Fc for bispecific antibody production, Oncotarget 8 (31) (2017) 51037–51049.
[22] T. Schlothauer, S. Herter, C.F. Koller, S. Grau-Richards, V. Steinhart, C. Spick, M. Kubbies, C. Klein, P. Umaña, E. Mössner, Novel human IgG1 and IgG4 Fc-engineered antibodies with completely abolished immune effector functions, Protein Eng. Des. Sel. 29 (10) (2016) 457–466.
[23] T. Dao, S. Yan, N. Veomett, D. Pankov, L. Zhou, T. Korontsvit, A. Scott, J. Whitten, P. Maslak, E. Casey, T. Tan, H. Liu, V. Zakhaleva, M. Curcio, E. Doubrovina, R. J. O'Reilly, C. Liu, D.A. Scheinberg, Targeting the intracellular WT1 oncogene product with a therapeutic human antibody, Sci. Transl. Med. 5 (176) (2013) 176ra33.
[24] S.M. Swain, M.S. Ewer, G. Viale, S. Delaloge, J.M. Ferrero, M. Verrill, R. Colomer, C. Vieira, T.L. Werner, H. Douthwaite, D. Bradley, M. Waldron-Lynch, A. Kiermaier, J. Eng-Wong, C. Dang, Pertuzumab, trastuzumab, and standard anthracycline- and taxane-based chemotherapy for the neoadjuvant treatment of patients with HER2-positive localized breast cancer (BERENICE): a phase II, open-label, multicenter, multinational cardiac safety study, Ann. Oncol. 29 (3) (2018) 646–653.
[25] R. Arora, M. Kisiel, C. MacColl, Panitumumab-induced pulmonary toxicity, Curr. Oncol. 26 (5) (2019) e700–e702.
[26] E. Jäger, Y.T. Chen, J.W. Drijfhout, J. Karbach, M. Ringhoffer, D. Jäger, M. Arand, H. Wada, Y. Noguchi, E. Stockert, L.J. Old, A. Knuth, Simultaneous humoral and cellular immune response against cancer-testis antigen NY-ESO-1: definition of human histocompatibility leukocyte antigen (HLA)-A2-binding peptide epitopes, J. Exp. Med 187 (2) (1998) 265–270.
[27] A. Raza, M. Merhi, V.P. Inchakalody, R. Krishnankutty, A. Relecom, S. Uddin, S. Dermime, Unleashing the immune response to NY-ESO-1 cancer testis antigen as a potential target for cancer immunotherapy, J. Transl. Med 18 (1) (2020) 140.
[28] M.A. Purbhoo, D.H. Sutton, J.E. Brewer, R.E. Mullings, M.E. Hill, T.M. Mahon, J. Karbach, E. Jäger, B.J. Cameron, N. Lissin, P. Vyas, J.L. Chen, V. Cerundolo, B. K. Jakobsen, Quantifying and imaging NY-ESO-1/LAGE-1-derived epitopes on tumor cells using high affinity T cell receptors, J. Immunol. 176 (12) (2006) 7308–7316.
[29] R. Thomas, G. Al-Khadairi, J. Roelands, W. Hendrickx, S. Dermime, D. Bedognetti, J. Decock, NY-ESO-1 based immunotherapy of cancer: current perspectives, Front. Immunol. 9 (2018) 947.
[30] S. Mundlos, J. Pelletier, A. Darveau, M. Bachmann, A. Winterpacht, B. Zabel, Nuclear localization of the protein encoded by the Wilms' tumor gene WT1 in embryonic and adult tissues, Development 119 (4) (1993) 1329–1341.
[31] W.B. Zhao, Y. Shen, W.H. Liu, Y.M. Li, S.J. Jin, Y.C. Xu, L.Q. Pan, Z. Zhou, S. Q. Chen, Soluble expression of Fc-fused T cell receptors allows yielding novel bispecific T cell engagers, Biomedicines 9 (7) (2021) 790.
[32] M. Ferez, M. Castro, B. Alarcon, H.M. van Santen, Cognate peptide-MHC complexes are expressed as tightly apposed nanoclusters in virus-infected cells to allow TCR crosslinking, J. Immunol. 192 (1) (2014) 52–58.
[33] R. Lindstedt, N. Monk, G. Lombardi, R. Lechler, Amino acid substitutions in the putative MHC class II "dimer of dimers" interface inhibit CD4+ T cell activation, J. Immunol. 166 (2) (2001) 800–808.
[34] J.D. Colbert, F.M. Cruz, C.E. Baer, K.L. Rock, Tetraspanin-5-mediated MHC class I clustering is required for optimal CD8 T cell activation, Proc. Natl. Acad. Sci. USA 119 (42) (2022), e2122188119.
[35] J.A. Engelman, K. Zejnullahu, T. Mitsudomi, Y. Song, C. Hyland, J.O. Park, N. Lindeman, C.M. Gale, X. Zhao, J. Christensen, T. Kosaka, A.J. Holmes, A. M. Rogers, F. Cappuzzo, T. Mok, C. Lee, B.E. Johnson, L.C. Cantley, P.A. Jänne, MET amplification leads to gefitinib resistance in lung cancer by activating ERBB3 signaling, Science 316 (5827) (2007) 1039–1043.
[36] M.X. Sliwkowski, G. Schaefer, R.W. Akita, J.A. Lofgren, V.D. Fitzpatrick, A. Nuijens, B.M. Fendly, R.A. Cerione, R.L. Vandlen, K.L. Carraway 3rd, Coexpression of ErbB2 and ErbB3 proteins reconstitutes a high affinity receptor for heregulin, J. Biol. Chem. 269 (20) (1994) 14661–14665.
[37] M. Bacac, S. Colombetti, S. Herter, J. Sam, M. Perro, S. Chen, R. Bianchi, M. Richard, A. Schoenle, V. Nicolini, S. Diggelmann, F. Limani, R. Schlenker, T. Hüsser, W. Richter, K. Bray-French, H. Hinton, A.M. Giusti, A. Freimoser-Grundschober, L. Lariviere, C. Neumann, C. Klein, P. Umaña, CD20-TCB with obinutuzumab pretreatment as next-generation treatment of hematologic malignancies, Clin. Cancer Res 24 (19) (2018) 4785–4797.
[38] Z. Wu, N.V. Cheung, T cell engaging bispecific antibody (T-BsAb): from technology to therapeutics, Pharmacol. Ther. 182 (2018) 161–175.
[39] E. Seung, Z. Xing, L. Wu, E. Rao, V. Cortez-Retamozo, B. Ospina, L. Chen, C. Beil, Z. Song, B. Zhang, M. Levit, G. Deng, A. Hebert, P. Kirby, A. Li, E.J. Poulton, R. Vicente, A. Garrigou, P. Piepenhagen, G. Ulinski, M. Sanicola-Nadel, D. S. Bangari, H. Qiu, L. Pao, D. Wiederschain, R. Wei, Z.Y. Yang, G.J. Nabel, A trispecific antibody targeting HER2 and T cells inhibits breast cancer growth via CD4 cells, Nature 603 (7900) (2022) 328–334.